Geosynthetics, J. Kuwano & J. Koseki (eds)

Parametric analysis of reinforced soil walls with different height and reinforcement stiffness

Bathurst, R.J.
GeoEngineering Centre at Queen's-RMC, Royal Military College of Canada, Kingston, Ontario, Canada
Hatami, K.
School of Civil Engineering and Environmental Science, University of Oklahoma, Norman, Oklahoma, USA

Keywords: Numerical modelling, FLAC, reinforced soil walls

ABSTRACT: In this paper a FLAC numerical code is used to investigate the influence of wall height and reinforcement stiffness on the behaviour of a series of otherwise nominally identical reinforced soil wall structures. The original code has been verified against the physical results of a series of 3.6 m-high modular block-faced (segmental) wall structures constructed at RMC. Three wall heights are investigated here (3.6, 6 and 9 m high) in combination with three different reinforcement materials corresponding to a weak polypropylene geogrid, a woven polyester geogrid and a very stiff welded wire mesh reinforcement product. The paper shows how construction-induced wall out-of-alignment varies with height and reinforcement stiffness. The numerical results demonstrate that as the height of the wall increases and/or reinforcement stiffness increases, the fraction of total earth force taken by the reinforcement layers (at the connections) increases and, conversely, the fraction carried by the restrained toe decreases. Hence, the influence of a horizontally restrained footing (toe) on load capacity is more pronounced for short walls than for taller walls.

1 INTRODUCTION

A total of 11 full-scale instrumented reinforced soil walls have been recently completed at the Royal Military College of Canada. The walls were 3.6 m in height and constructed with a column of solid modular concrete (segmental) units, wrapped-face or incremental concrete facing panels (Bathurst et al. 2002). The backfill soil in all cases was a clean uniform size sand and the structures were placed over a rigid foundation. The soil reinforcement was comprised of different arrangements of a weak biaxial polypropylene geogrid, woven polyester geogrid or welded wire mesh material. The matrix of test results has allowed a database of high-quality experimental results to be collected that can be used to isolate the contribution of wall facing type, reinforcement type and spacing to wall performance at working stress conditions (end of construction) and at conditions approaching collapse under uniform surcharge loading. Each of the structures was heavily instrumented to record horizontal and vertical toe boundary reactions, vertical earth pressures at the foundation, facing horizontal displacements, connection loads, and reinforcement strains.

The data from four different modular block retaining wall models in the physical testing program have been used to verify a numerical model using the program FLAC (Itasca 2005, Hatami and Bathurst 2005, 2006). In this paper, the same FLAC model is now used to investigate the influence of reinforcement stiffness and wall height on the end-of-construction behaviour of a series of modular block walls that are similar to the 3.6 m-high RMC structures that were used to verify the original FLAC code. The current numerical investigation extends previous simulation results to modular block walls with heights of 3.6, 6 and 9 m together with three different reinforcement products. Each wall was constructed with a maximum reinforcement spacing of 0.6 m and a target facing batter of 8 degrees from the vertical.

2 NUMERICAL MODELS

2.1 *General*

Figure 1 shows an example numerical model used in this study. Computations were carried out in large-strain mode to ensure sufficient accuracy in the event of large wall deformations or reinforcement strains and to accommodate the moving local datum as each row of facing units and soil layer was placed during construction simulation. Sequential bottom-up construction of each segmental wall model and compaction of the soil was numerically simulated

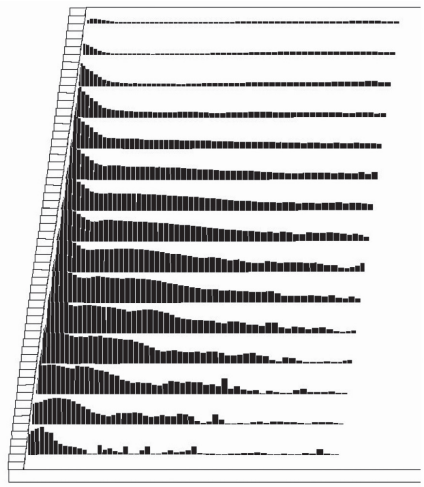

Figure 1. Example 9 m high modular block (segmental) retaining wall showing facing column and bar graphs of reinforcement loads at end of construction.

following the procedures described by Hatami and Bathurst (2005).

2.2 *Material properties*

The compacted backfill soil was modelled as a homogenous, isotropic, nonlinear elastic-perfectly plastic material with Mohr-Coulomb failure criterion and dilation angle (Itasca 2005). The sand backfill soil was modelled as a nonlinear elastic medium prior to peak strength using the stress-dependent hyperbolic model proposed by Duncan et al. (1980). However, the elastic modulus number of the soil (K_e) was increased by a factor of two from back-fitted triaxial test data to account for the increased stiffness of the soil due to plane strain boundary conditions (Hatami and Bathurst 2005). A small cohesion value was introduced in the soil model to prevent premature soil yielding in locally low confining pressure zones and to account for possible additional apparent cohesion due to moisture in the backfill soil. Soil properties are summarized in Table 1.

Three different soil reinforcement materials were considered in this investigation to cover a typical range of products used in reinforced soil walls (a polypropylene (PP) geogrid, a woven polyester (PET) geogrid, and a welded wire mesh grid (WWM). A generalized time-dependent reinforcement tangent stiffness function $J_t(\varepsilon, t)$ was used to characterise the load-strain-time properties of the reinforcement materials using an expression proposed by Hatami and Bathurst (2006):

$$J_t(\varepsilon, t) = \frac{1}{J_o(t)\left(\frac{1}{J_o(t)} + \frac{\eta(t)}{T_f(t)}\varepsilon\right)^2} \quad (1)$$

Table 1. Soil properties.

Property	Value
K_e (elastic modulus number)	2840
K_b (bulk modulus number)	1420
K_{ur} (unloading-reloading modulus number)	3410
n (elastic modulus exponent)	0.5
m (bulk modulus exponent)	0.5
R_f (failure ratio)	0.86
ν_t (tangent Poisson's ratio)	0 - 0.49
ϕ (peak friction angle) (degrees)	44
c (cohesion) (kPa)	2
ψ (dilation angle) (degrees)	11
γ (kN/m^3)	16.8

Table 2. Reinforcement properties.

Reinforcement type	Equation 1 and t = 1000 hours			Ultimate (index) strength
	J_o (t) (kN/m)	η(t)	T_f (t) (kN/m)	$T_y^{(1)}$ (kN/m)
PP	339	0.87	23.1	42
PET	171	0	NA	48
WWM	3100	0	NA	21

Notes: (1) Based on peak strength measured during 10% strain/minute constant-rate-of-strain (CRS) test; NA = not applicable for WWM case with $\eta(t) = 0$.

where: $J_o(t)$ is the initial tangent stiffness, $\eta(t)$ is a scaling function, $T_f(t)$ is the stress-rupture function for the reinforcement; and t is time. The values assumed in this study are given in Table 2 and correspond to a duration of loading of 1000 hours. The relative stiffness of the reinforcement materials increases in the order of PET, PP and WWM in this investigation.

The facing units were discrete solid masonry concrete units with a continuous shear key to transfer column loads and to assist with facing alignment during construction.

2.3 *Interfaces and boundary conditions*

The interfaces between dissimilar materials were modelled as linear spring-slider systems with interface shear strength defined by the Mohr-Coulomb failure criterion. The value of interface stiffness between modular blocks was selected to match physical test results from laboratory direct shear tests.

A fixed boundary condition in the horizontal direction was assumed at the numerical grid points on the backfill far-end boundary, representing the bulkheads that were used to contain the soil at the back of the RMC test facility. A fixed boundary condition in both horizontal and vertical directions was used at the foundation level matching the test facility concrete strong floor. The toe of the facing column was restrained horizontally by a very stiff spring element with properties matching those measured at this boundary in the RMC physical tests.

3 EXAMPLE RESULTS

Figure 2 shows normalized plots of the out-of-alignment of the facing column with respect to the target facing batter of 8 degrees from the vertical. Here z is elevation above the wall toe, Δx is horizontal wall displacement from the target position (i.e. if the blocks could be stacked without any lateral displacement) and H is the height of the wall. This out-of-alignment is a result of the cumulative slip that is generated at the interface between block units as the facing column is built up and the soil is placed and compacted behind the wall. In general, as the stiffness of the reinforcement decreases and/or the height of the wall increases, the relative out-of-alignment increases. These trends are highlighted in Figure 3a. The maximum relative out-of-alignment values are in the range of 0.5 to 0.8% of the wall height for the 9 m-high wall case. Figure 3b shows the relative location of the bulge in the out-of-alignment profiles below the wall crest for the six cases investigated. The plots show that the relative location of the bulge in wall out-of-alignment with respect to the bottom of the wall decreases with increasing wall height and increasing reinforcement stiffness.

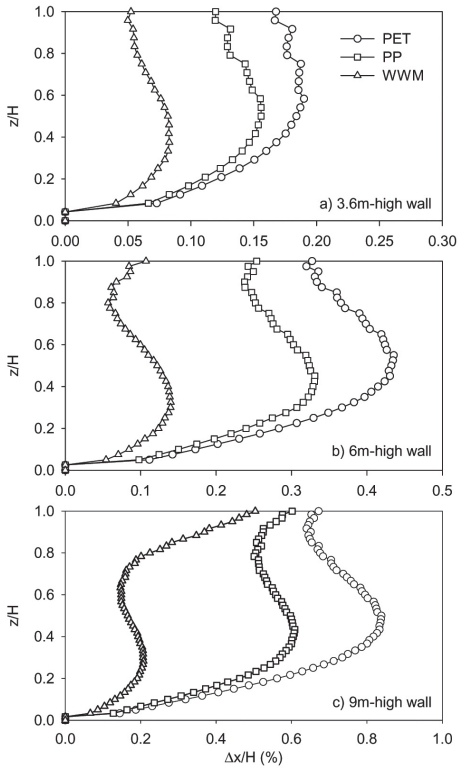

Figure 2. Normalized facing column out-of-alignment.

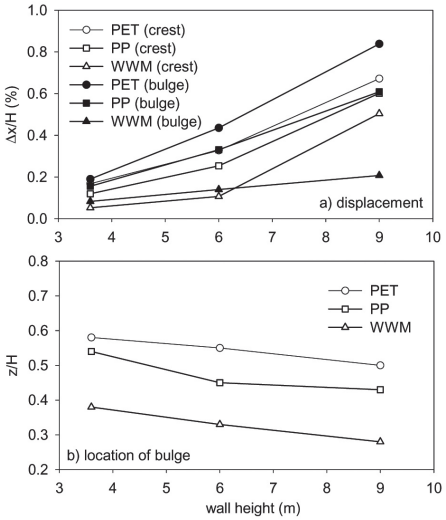

Figure 3. Normalized maximum crest out-of-alignment, facing bulge and bulge location at end of construction.

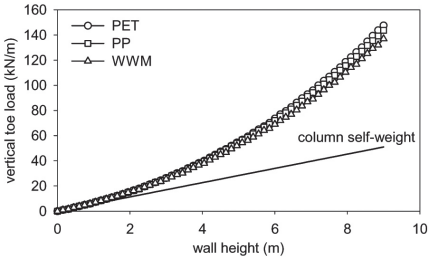

Figure 4. Vertical toe load versus height of wall.

Figure 4 shows the evolution of the vertical toe load as the height of the facing column increases. The data show that the vertical footing load is generally well in excess of the vertical toe load due to self-weight of the facing column alone. The difference is due to downdrag forces generated at the reinforcement connections as the wall facing column moves out and the soil moves down behind the wall. The elevated reinforcement loads due to downdrag are evident in the reinforcement tensile load distributions plotted in Figure 1. Importantly, the magnitude of the vertical toe load is sensibly independent of reinforcement stiffness.

Figure 5 shows the magnitude and distribution of connection and toe loads computed at the wall facing column. The data show that in each case the toe load is significant in comparison to the individual reinforcement layer loads. In Figure 5a the distribution of connection loads approaches a triangular shape with depth below the crest of the wall for the stiffest reinforcement case. However, this trend does not persist for the taller walls.

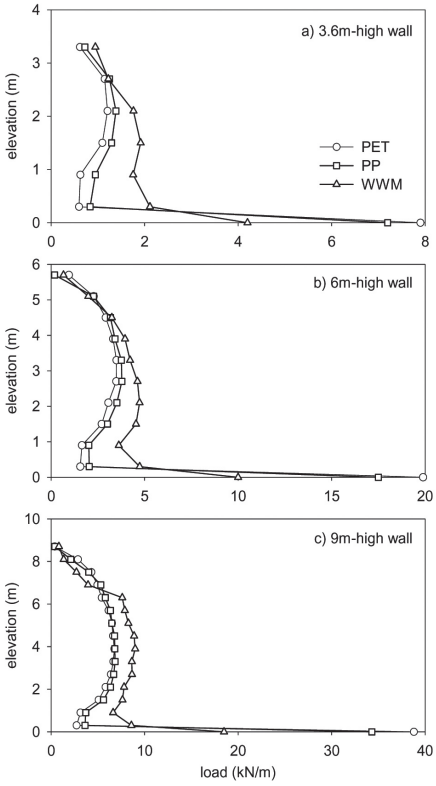

Figure 5. Connection and toe loads.

The relative contribution of the horizontally restrained toe to resist the total horizontal earth force acting on the facing column is summarized in Figure 6. The data show that as the wall height increases and/or the reinforcement stiffness increases, the contribution of the toe to horizontal load capacity of the wall decreases. In other words, the contribution of the rigid foundation in combination with a horizontally restrained toe is more pronounced for shorter walls than higher walls when all other factors remain the same.

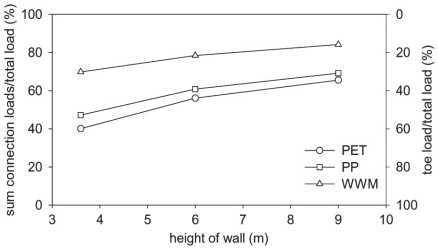

Figure 6. Contribution of sum of reinforcement connection loads and toe load to total horizontal earth force.

4 CONCLUSIONS

In this paper, a verified numerical code using the program FLAC has been used to explore the influence of height and reinforcement stiffness on the end-of-construction behaviour of a series of modular block reinforced soil walls. The numerical results demonstrate that, as the height of the wall decreases and/or reinforcement stiffness decreases, the ratio of the lateral earth load carried by the horizontally restrained toe at the base of a structural facing column to that carried by the reinforcement layers increases.

REFERENCES

Bathurst, R.J. Walters, D.L., Hatami, K., Saunders, D.D., Vlachopoulos, N., Burgess, G.P. and Allen, T.M. (2002). "Performance Testing and Numerical Modelling of Reinforced Soil Retaining Walls", 7th International Geosynthetics Conf., Nice, France, Vol. 1, pp. 217-220.

Duncan, J.M., Byrne, P., Wong, K.S. and Mabry, P. (1980). "Strength, Stress-strain and Bulk Modulus Parameters for Finite-element Analysis of Stresses and Movements in Soil Masses". Report No. UCB/GT.

Hatami, K. and Bathurst, R.J. (2005). "Development and Verification of a Numerical Model for the Analysis of Geosynthetic Reinforced Soil Segmental Walls under Working Stress Conditions", Canadian Geotechnical Journal, Vol. 42, No. 4, pp. 1066-1085.

Hatami, K. and Bathurst, R.J. (2006). "A Numerical Model for Reinforced Soil Segmental Walls under Surcharge Loading", Journal of Geotechnical and Geoenvironmental Engineering, ASCE, (in press).

Itasca Consulting Group. (2005). FLAC—Fast Lagrangian Analysis of Continua. Version 5.00. Itasca Consulting Group Inc., Minneapolis, Minnesota.